NASA TECHNICAL TRANSLATION NASA TT F-15,953

EFFECT OF ARTIFICIAL STABILITY ON AIRCRAFT PERFORMANCE

D. Reich

Translation of "Einfluss der künstlichen Stabilität auf die Flugleistungen," in Forderungen an Flugregelanlagen und Auslegungs-Probleme unter besonderer Berücksichtigung der Flugmechanik, Deutsche Gesellschaft für Luft- und Raumfahrt, Cologne, West Germany, DLR-MITT-72-05, March 1972, pp. 171-186

NATIONAL AERONAUTICS AND SPACE ADMINISTRATION
WASHINGTON, D.C. 20546 SEPTEMBER 1974

STANDARD TITLE PAGE

1. Report No. NASA TT F-15,953	2. Government Accession No.	3. Recipient's Catalog No.
4. Title and Subtitle EFFECT OF ARTIFICIAL STABILITY ON AIRCRAFT PERFORMANCE		5. Report Date September 1974 6. Performing Organization Code
7. Author(s) D. Reich, Messerschmitt-Bölkow-Blohm GmbH, Ottobrunn, West Germany		8. Performing Organization Report No. 10. Work Unit No.
9. Performing Organization Name and Address Leo Kanner Associates, P.O. Box 5187, Redwood City, California 94063		11. Contract or Grant No. NASw-2481 13. Type of Report and Period Covered Translation
12. Sponsoring Agency Name and Address NATIONAL AERONAUTICS AND SPACE ADMINISTRATION, WASHINGTON, D.C. 20546		14. Sponsoring Agency Code

15. Supplementary Notes
Translation of "Einfluss der künstlichen Stabilität auf die Flugleistungen," in Forderungen an Flugregelanlagen und Auslegungs-Probleme unter besonderer Berücksichtigung der Flugmechanik, Deutsche Gesellschaft für Luft- und Raumfahrt, Cologne, West Germany, DLR-MITT-72-05, March 1972, pp. 171-186.

16. Abstract Based on the control configured vehicle (CCV) concept, i.e. taking account of flight control during the design phase, the effect of an artificial longitudinal stability on the performance of aircraft was investigated. In consequent application of the CCV concept, in the most favorable cases a decrease of about 15% in takeoff weight (for the same radius of action) or an increase of 11% in radius of action (for the same takeoff weight) can be achieved. For a fighter aircraft, it is shown that the advantages of artificial longitudinal stability are obtained for high lift coefficients and for plane wing-body drag polars.

17. Key Words (Selected by Author(s))	18. Distribution Statement Unclassified - Unlimited

19. Security Classif. (of this report)	20. Security Classif. (of this page)	21. No. of Pages	22. Price
Unclassified	Unclassified	14	

NASA-HQ

Table of Contents

EFFECT OF ARTIFICIAL STABILITY ON AIRCRAFT PERFORMANCE *

D. Reich
Messerschmitt-Bölkow-Blohm GmbH, Ottobrunn, West Germany

1. CCV Concepts /171**

For the past several years, efforts have been made in the international aviation industry to make use of the possibilities of automatic flight control in a somewhat more consistent manner. Until now, the task of automatic flight control was to eliminate shortcomings which were put up with in favor of certain advantages in an aircraft (cf. the "dutch roll" in the case of the Boeing 707) or to relieve the pilot (autopilot).

Incorporation of the flight control system into the design /172 cycle as shown in Fig. 1 led to concepts which have become known under the name CCV (control configured vehicle) in English-speaking areas. Figure 2 shows a list of such concepts. If various CCV concepts are applied consistently, we can achieve about a 15% reduction in takeoff weight (for a given range) or an increase in range (for a given takeoff weight) of 11% in the most favorable case, as shown in Fig. 3. The data shown here have been taken from a corresponding study by the Boeing Company.

The rest of this paper will be concerned only with the enhancement of performance obtained by sacrificing inherent static longitudinal stability.

---

*The results presented in this paper have been taken from a corresponding Messerschmitt-Bölkow-Blohm study ("Jet-controlled combat aircraft," Volume 2, Configurations and Flight Performance, MBB Report No 791-2-71).

**Numbers in the margin indicate pagination in the foreign text.

2. Static Longitudinal Stability and Trim Drag

As can be seen from Fig. 4, trim drag consists of the following components:

a) the portion resulting from increased and reduced loads on the wing produced by the elevator;

b) the induced drag of the elevator, and

c) the downwash components associated with elevator lift.

By shifting lift from the wing to the elevator, we obtain the optimal distribution of elevator lift and total lift shown in Fig. 5 under simplifying conditions for given elevator/wing area ratios. The plotted stability limits show the order of /173 magnitude of drag gains which are to be obtained by applying stability requirements. The curve optimum in Fig. 5 is shifted toward smaller elevator/total lift ratios by tilting the elevator lift vector here, taking downwash behind the wing into consideration, as shown in Fig. 6 using a drag polar.

Figure 7 shows the relationship between static longitudinal stability and the elevator lift necessary for trim. It should be noted here that, as shown, the expression $\Delta x/\ell\mu$, employed in the rest of this paper, is not identical to the stability index $\partial c_M/\partial c_A$. The effect of the center of gravity position on induced drag is shown in Fig. 8. The values in this graph apply to a special design, shown in Fig. 11. Flight conditions of altitude = = 0, Mach number = 0.8 and load factor N = 5 represent an arbitrary high-lift condition. With a center of gravity position of $\Delta x/\ell\mu$ = = 0.02, the aircraft behaves neutrally. If the aircraft's center of gravity is shifted aftward, the elevator receives more and more lift, while the wing is relieved and operates with a more favorable lift coefficient for its polars. The additional induced drag on the elevator reduces this effect to a greater and greater extent as its fraction of total lift increases.

Figures 9 and 10 demonstrate -- on the basis of wind-tunnel data -- the increases in drag and lift accompanying a change in the stability index. A series of measurements were made at various angles of attack and elevator longitudinal dihedral angles, and those results were combined which produced moment equilibrium at the three given reference points (centers of gravity). The model used was a configuration corresponding to that shown in Fig. 11. /174

3. Enhancement of the Performance of Given Aircraft

Figure 11 shows two views of a basic configuration used for performance and weight analysis. Pronounced wing sweepback, a two-stage intake and an afterburner give this aircraft supersonic capabilities. Good maneuverability in the subsonic region is made possible by low surface loading and a high thrust-to-weight ratio.

Considerable trim-drag reduction by shifting the center of gravity can be achieved in flight states with high load factors (Fig. 12). For flight at 1 g, in which induced drag plays a subordinate role, the gains are insignificant. The variation in maximum load factor with center of gravity position is shown in Fig. 13.

Specific holding time and "curve(d) climb" capability are shown in Figs. 14 and 15. Lines of constant elevator volume are plotted as parameters in both figures. It is found that in the case of "curve(d) climb" capability, the effect of the size of the elevator (elevator volume) is relatively small. The reason for this lies in the small percentage of detrimental drag out of total drag for high lift coefficients. Figure 16 summarizes the results of the preceding studies, among other things.

4. Weight Gains in New Designs

/175

The adaptation of an aircraft design to given maneuver performance is primarily accomplished via power plant thrust and wing size. In the case at hand, maneuvering conditions are represented by a 1-g supersonic and a 4-g subsonic case (Fig. 17). On the right branch of a curve, the aircraft is dimensioned on the basis of subsonic requirements; supersonic requirements are over-satisfied as the result of high surface loading. At the break in the curve, dimensioning is based on both types of requirements simultaneously. The best takeoff weights are obtained with increasing displacement of the center of gravity aftward and higher surface loads. It should be noted that all designs have been laid out for the same mission radius of 150 nautical miles. Figure 18 shows the summarized results of a configuration study. In each case, the minimum takeoff weights of three different configuration types have been plotted over the stability index $\partial c_M / \partial c_A$. An important outcome of this study is the different reactions of the three configurations to a change in static longitudinal stability. The "tail" aircraft is aerodynamically superior to the delta and canard configurations because of its wing design (larger aspect ratio). It flies with a more favorable drag/lift ratio to satisfy maneuvering requirements, due to its better polars. When the stability index is varied by a given amount, the percentage gain in drag is smaller for the aerodynamically superior configuration.

5. Summary

The advantages of artificial longitudinal stability are made use of primarily with high lift coefficients, the more so /176
the flatter the wing-body drag polar. The most important results of the performance and weight analysis described above are summarized in Fig. 19.

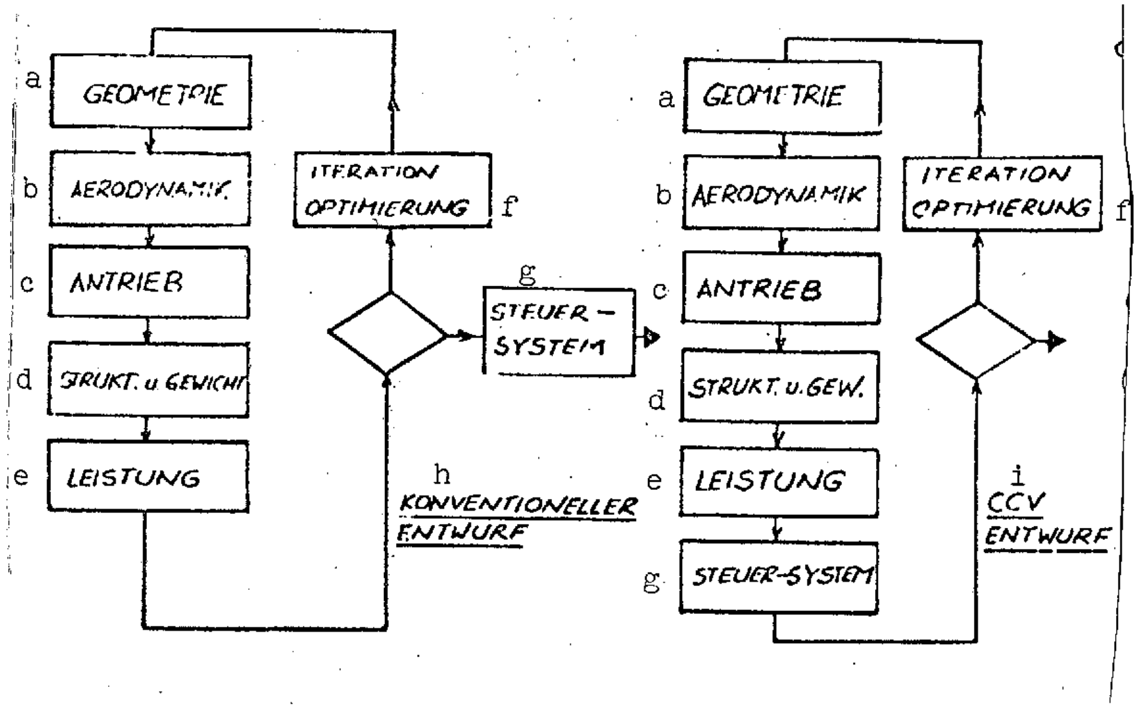

Fig. 1. Design cycle.

Key:
- a. Geometry
- b. Aerodynamics
- c. Propulsion
- d. Structure and weight
- e. Power/performance
- f. Optimization
- g. Control system
- h. Conventional design
- i. CCV design

- o Performance enhanced by dispensing with inherent stability
- o Improvement of flight characteristics: Direct lift control; Precision flight; All-weather flight; Autom. flight management
- o Reduction of timewise structural loads
- o Suppression of flutter
- o Gust reduction (ride smoothing)

Fig. 2. CCV concepts.

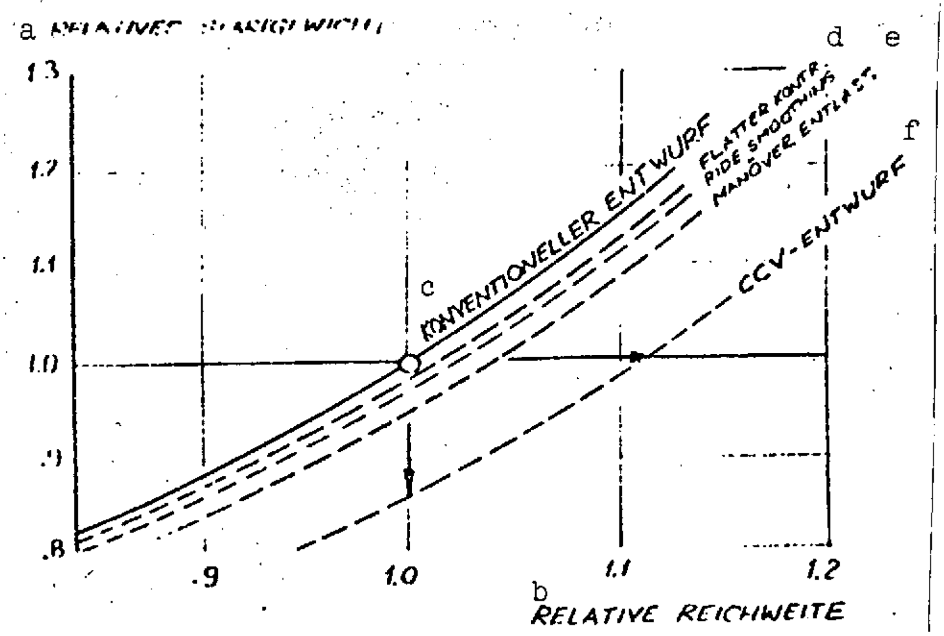

Fig. 3. CCV advantages for large transport aircraft.

Key: a. Relative takeoff weight
b. Relative range
c. Conventional design
d. Flutter control
e. Maneuver load relief
f. CCV design

$$C_{W_{TRIM}} = \underbrace{-\bar{C}_{AH}\left(\frac{F_H \cdot q_H}{F \cdot q}\right)\left(\frac{\Delta C_W}{\Delta C_A}\right)_{F.R.}}_{\text{Wing component}} + \left(\frac{F_H \cdot q_H}{F \cdot q}\right)\left(\underbrace{\frac{\bar{C}_{AH}^{2}}{\pi \cdot \Lambda_H}}_{\text{Induced elevator drag}} + \underbrace{\bar{C}_{A_H} * \sin\varepsilon}_{\text{Elevator downwash component}}\right)$$

$\bar{C}_{AH}$ — Elevator lift coefficient
F_H — Elevator area
q_H — Stagnation pressure at elevator
F — Wing area
q — Stagnation pressure at wing
$\left(\frac{\Delta C_W}{\Delta C_A}\right)_{F.R.}$ — Change in wing-body drag with the lift coefficient
Λ_H — Elevator aspect ratio
ε — Downwash angle

Fig. 4. Trim drag.

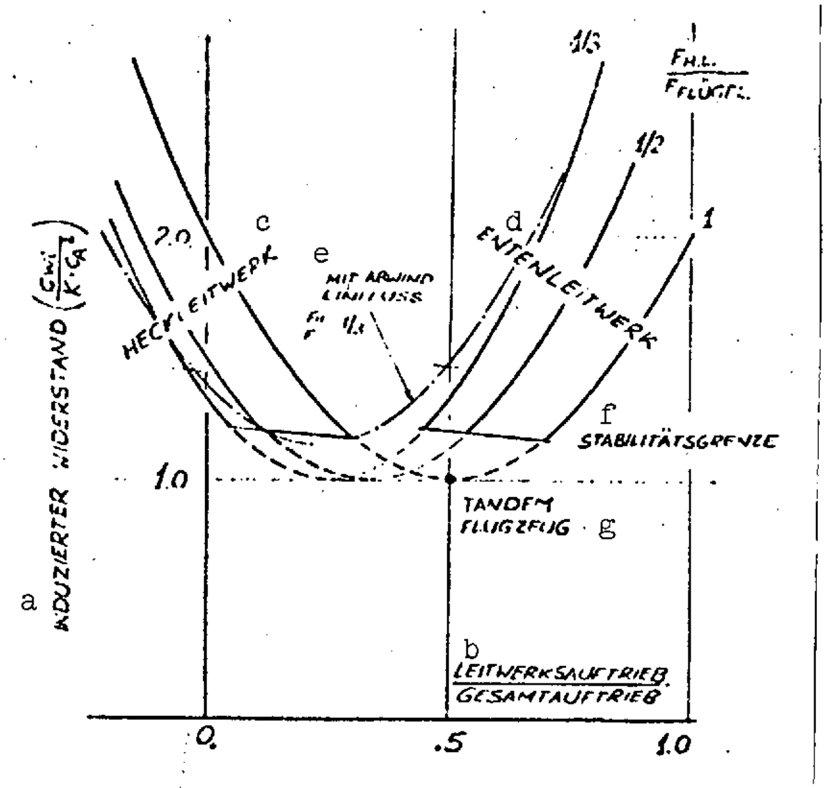

Fig. 5. Reduction of induced drag.

Key: a. Induced drag
b. (Elevator lift)/(total lift)
c. Tail elevator
d. Canard elevator
e. With downwash effect
f. Limit of stability
g. Tandem aircraft

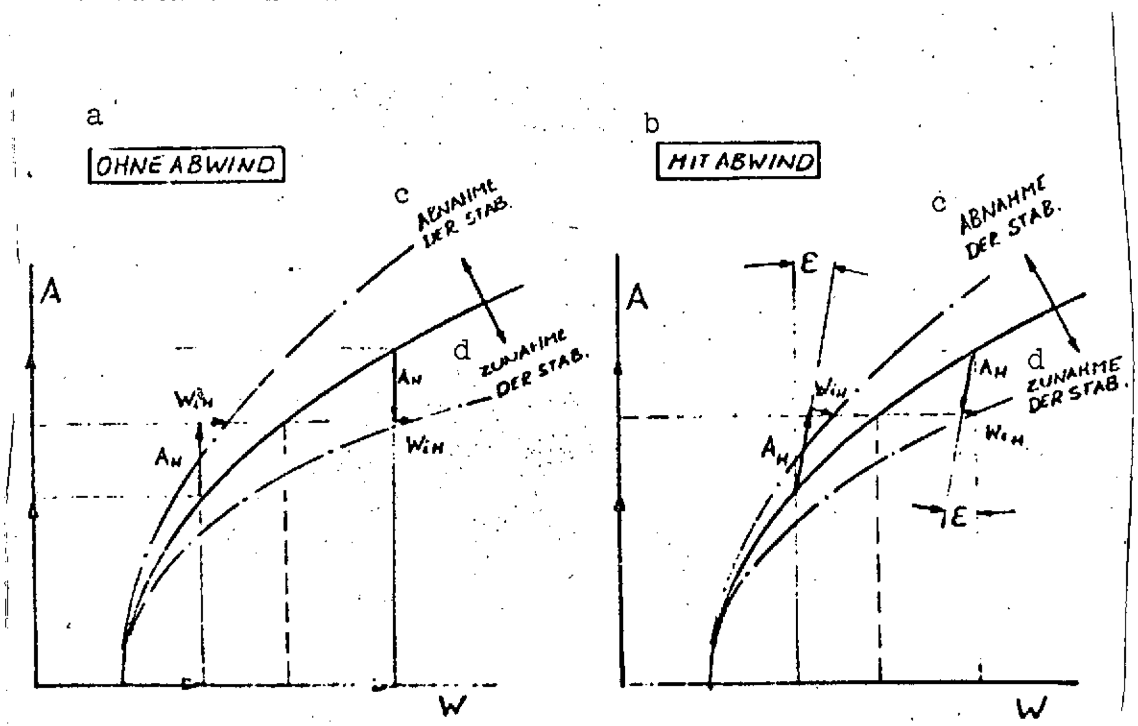

Fig. 6. Downwash effect.

Key: a. Without downwash
b. With downwash
c. Reduced stability
d. Increased stability
A = lift
W = drag
H = elevator

$$C_{A_H} = C_{A_{tr}} - \frac{C_{A_{tr}} - \dfrac{C_{M0}}{(l_H/l_\mu) + (\Delta x/l_\mu)}}{1 + \dfrac{(\partial C_M/\partial C_A)_{FR} - (\Delta x/l_\mu)}{((l_H/l_\mu) + (\Delta x/l_\mu))}}$$

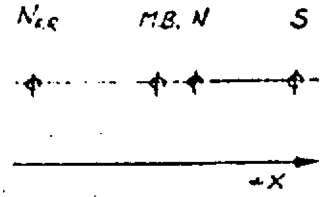

C_{A_H} -- Elevator lift coefficient

$C_{A_{TR}}$ Total lift coefficient

C_{M0} -- Zero-moment coefficient

l_H — Elevator lever arm

Δx $X_{M.B.} - X_S$ ~ CG position

l_μ ... Mean aerodynamic chord

$(\partial C_M/\partial C_A)_{FR} = \dfrac{X_{N_{FR}} - X_S}{l_\mu}$ ~ Stability index of wing-body combination

$\partial C_M/\partial C_A = \dfrac{X_N - X_S}{l_\mu}$ -- Stability index for overall configuration

N_{FR} – Wing-body neutral pt.

M.B. – Moment ref. pt.

N – Aircraft neutral pt.

S – Center of gravity

Fig. 7. Stability and elevator lift.

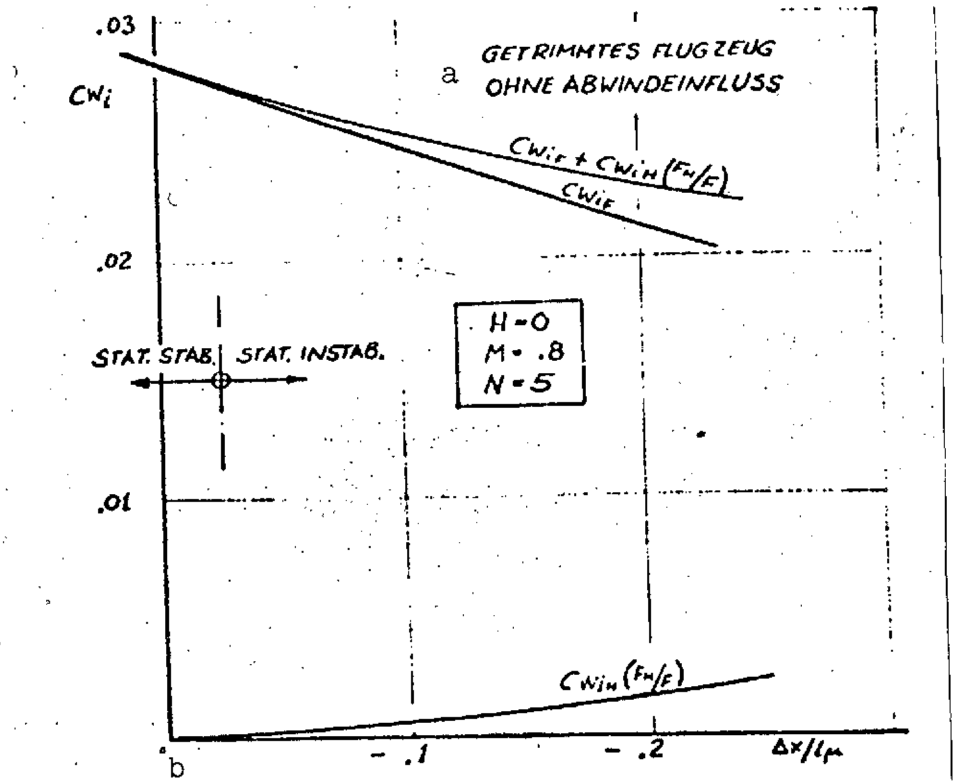

Fig. 8. Effect of CG position on induced drag.

Key: a. Trimmed aircraft without downwash effect
b. Distance between moment reference point and center of gravity

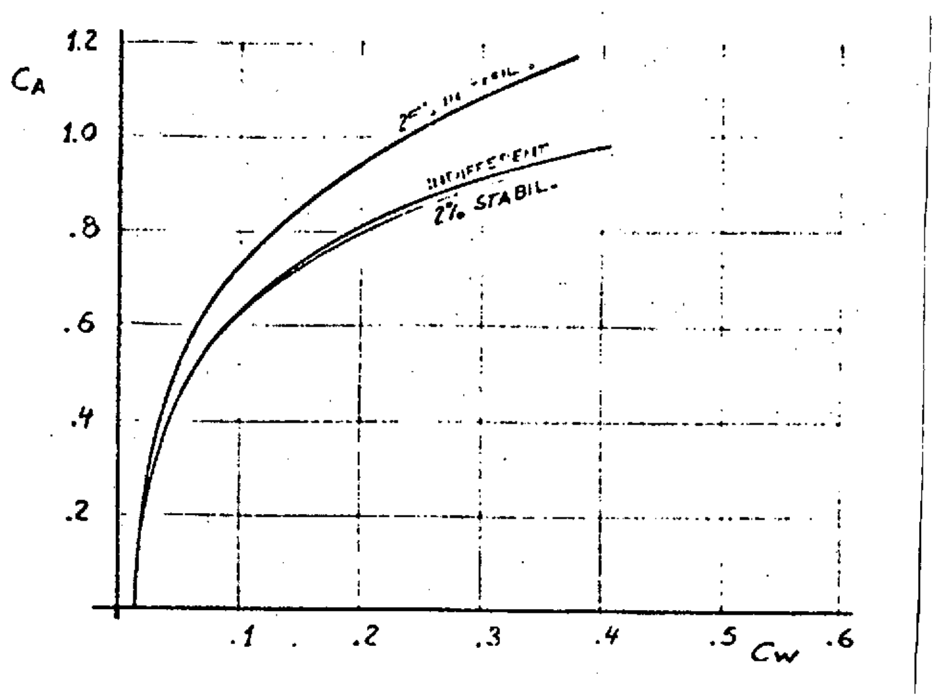

Fig. 9. Drag polar with change in stability index (measured).

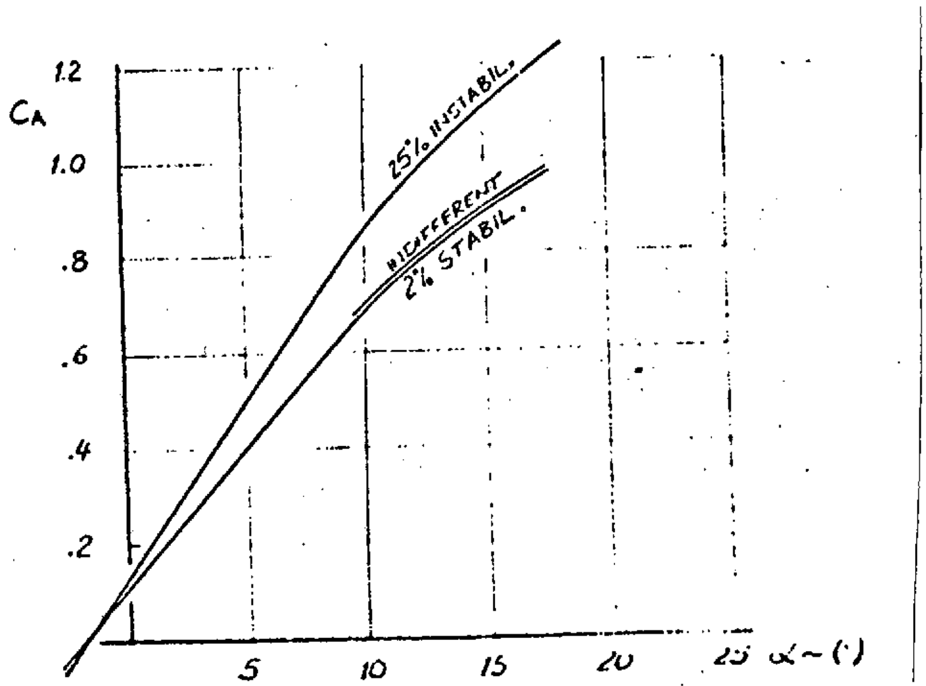

Fig. 10. Lift characteristic with change in stability index (measured).

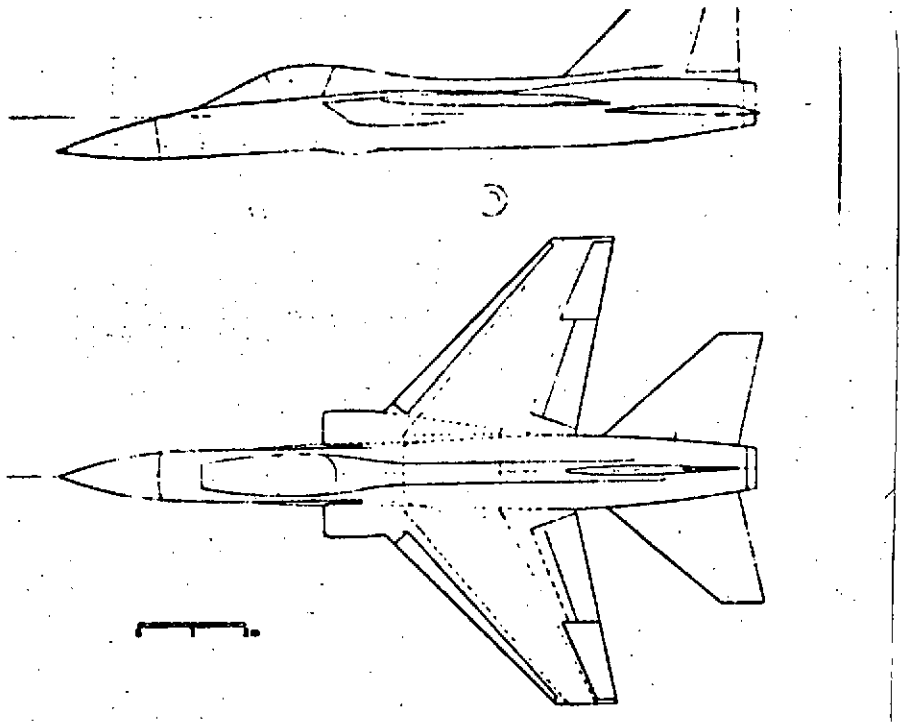

Fig. 11. Basic configuration.

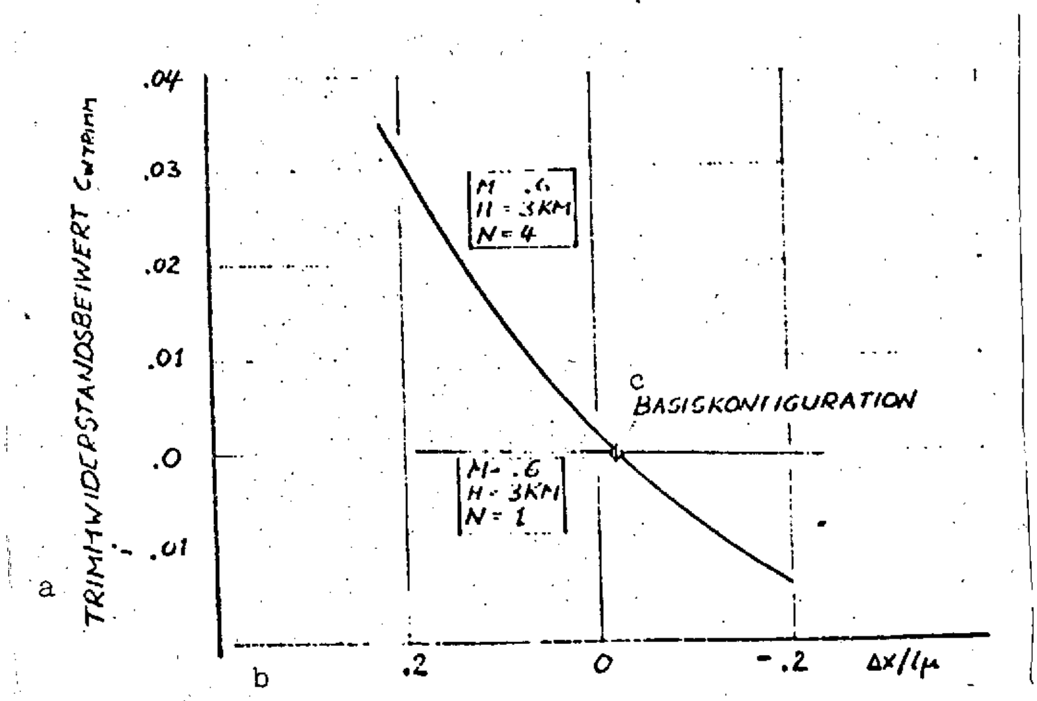

Fig. 12. Effect of CG position on trim drag.

Key: a. Trim drag coefficient
b. Distance between moment reference point and center of gravity
c. Basic configuration

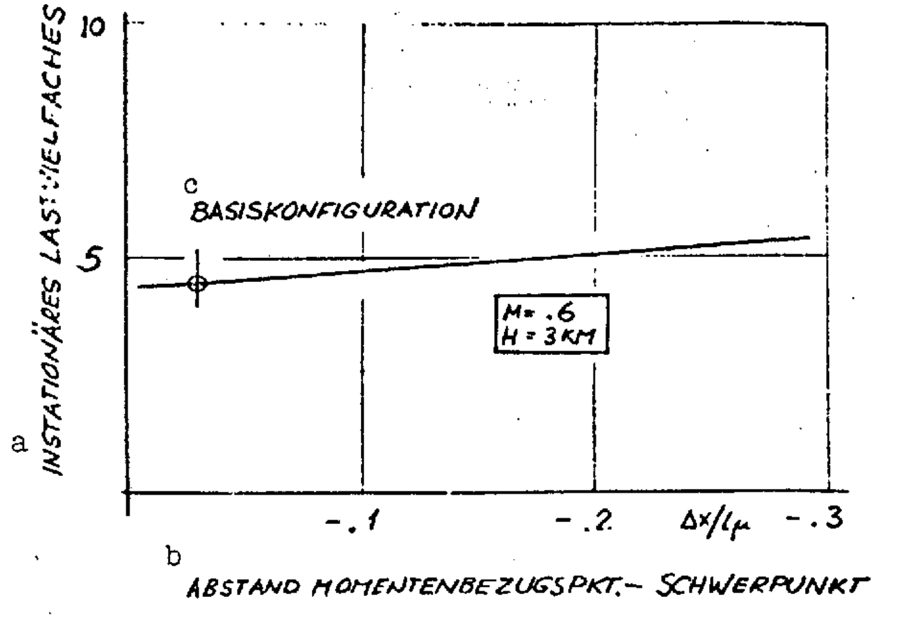

Fig. 13. Effect of CG position on nonsteady load factor.

Key: a. Nonsteady load factor
b. Distance between moment reference point and center of gravity
c. Basic configuration

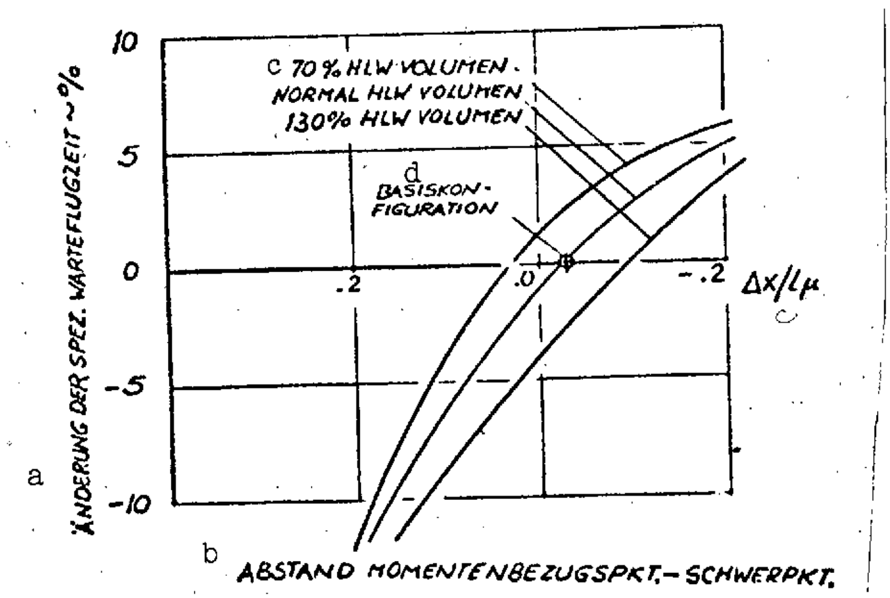

Fig. 14. Effect of CG position on specific holding time.

Key: a. Change in specific holding time
b. Distance between moment reference point and center of gravity
c. 70%, normal and 130% elevator volume
d. Basic configuration

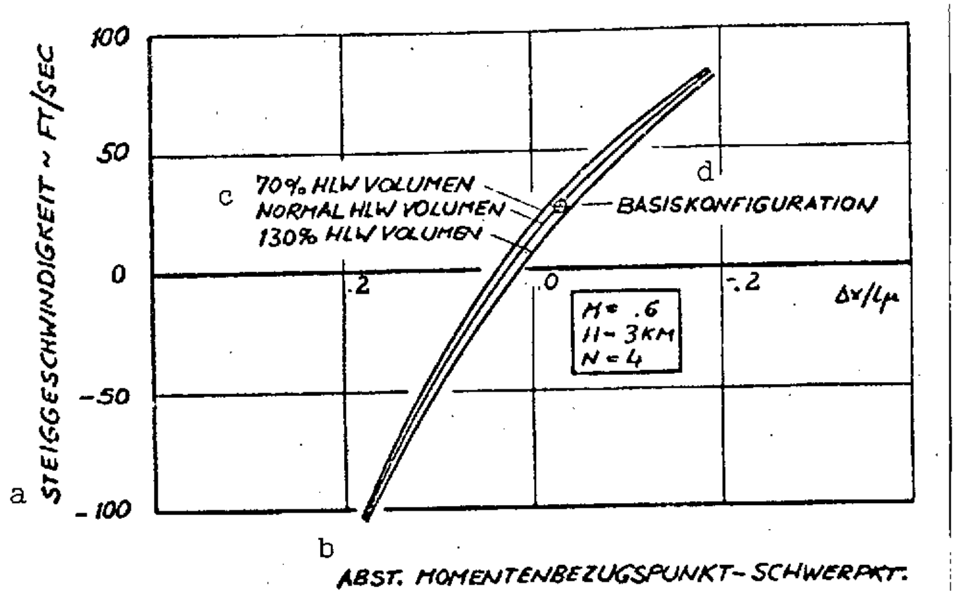

Fig. 15. Effect of CG position on rate of climb.

Key: a. Rate of climb
b. Distance between moment reference point and center of gravity
c. 70%, normal and 130% elevator volume
d. Basic configuration

	$\frac{\Delta x}{l\mu} = -.03$	$\frac{\Delta x}{l\mu} = -.20$
RELATIVE Specific Range	100%	101.5 %
RELATIVE MAX. load factor M = .6	100%	123%
Rate of climb ~ FT/S M = .6, N = 4g	25	83
Rate of climb ~ FT/S M = .9, N = 6g	84	173
Rate of climb ~ FT/S M = 1.6, N = 1g	-12	-1

Fig. 16. Performance enhancement by artifical stability.

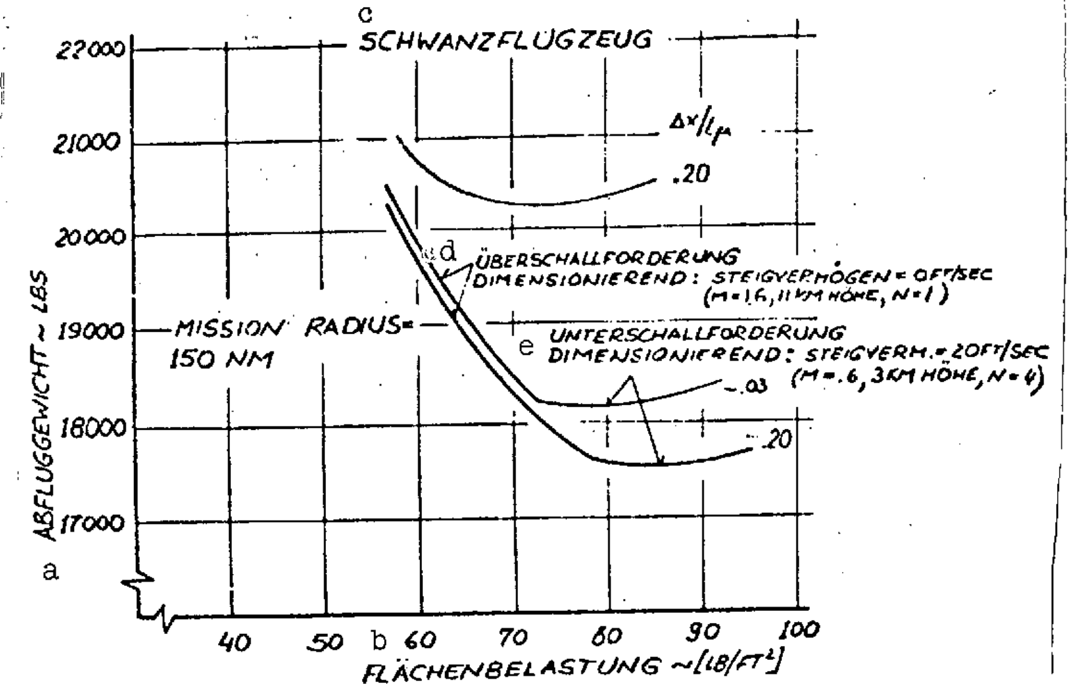

Fig. 17. Effect of surface loading and CG position on takeoff weight.

Key: a. Takeoff weight
b. Area loading
c. "Tail" aircraft
d. Dimensioned by supersonic requirements: climbing capability = ...
e. Dimensioned by subsonic requirements: climbing capability = ...

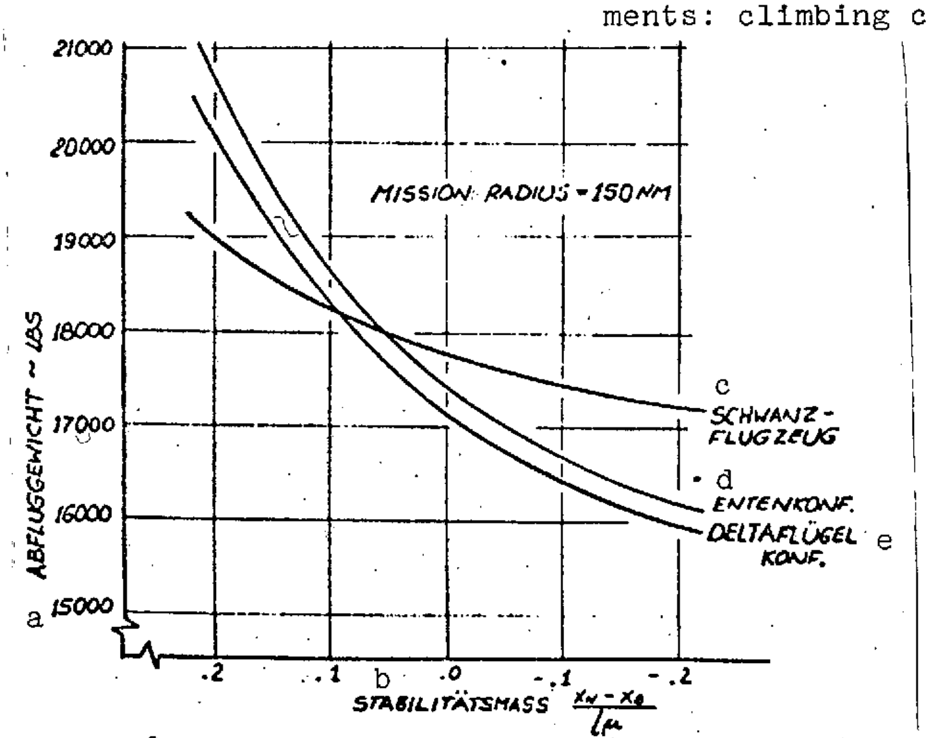

Fig. 18. Effect of stability index on minimum takeoff weight.

Key: a. Takeoff weight
b. Stability index
c. "Tail" aircraft
d. Canard configuration
e. Delta configuration

By applying the principle of artificial stability, it is possible to achieve the following improvements with an instability index of 20%:

- Drag, 15-20%
- Climbing capability with high load factors, 60-100 ft/sec
- Maximum load factor, ∿20%
- Takeoff weight with new design, 5-10%

Fig. 19.